

Exploring the disc/jet interaction in the radio-loud quasar 4C +74.26 with Suzaku

J. Larsson ^{1*}, A. C. Fabian ¹, D. R. Ballantyne ² and G. Miniutti ^{1,3}

¹*Institute of Astronomy, University of Cambridge, Madingley Road, Cambridge CB3 0HA*

²*Department of Physics, The University of Arizona, 1118 E. 4th Street, Tucson, Arizona 85721 USA*

³*Laboratoire Astroparticule et Cosmologie (APC), UMR 7164, 10 Rue A. Domon et L. Duquet, 75205 Paris, France*

Accepted 2008 May 21. Received 2008 May 15; in original form 2008 April 8

ABSTRACT

We report on a 90 ks *Suzaku* observation of the radio-loud quasar 4C +74.26. The source was observed in its highest flux state to date, and we find that it brightened by about 20 per cent during the observation. We see evidence of spectral hardening as the count rate increases and also find that the rms variability increases with energy up to about 4 keV. We clearly detect a broadened Fe line but conclude that it does not require any emission from inside about 50 r_g , although a much smaller inner radius cannot be ruled out. The large inner radius of our best fit implies that the inner disc is either missing or not strongly illuminated. We suggest that the latter scenario may occur if the power-law source is located high above the disc, or if the emission is beamed away from the disc.

Key words: galaxies: active – galaxies: individual: 4C +74.26 – X-rays: galaxies.

1 INTRODUCTION

Only a minority of active galactic nuclei (AGN) harbour relativistic radio-jets. The mechanism that drives the jet production in these radio-loud objects is unknown and constitutes an important issue in the study of accreting black holes. As both jets and X-ray emission originate close to the central black hole, it is clear that insight into this problem can be gained by comparing the X-ray properties of radio-loud and radio-quiet objects (see Ballantyne 2007 for a recent review).

Such studies of radio-loud and radio-quiet AGN, as well as Galactic black holes in their different states, have shown that radio-loud objects generally have weaker reflection features (as measured by the Fe $K\alpha$ line and Compton hump) and narrower Fe lines than their radio-quiet counterparts (see e.g. Woźniak et al. 1998; Eracleous, Sambruna & Mushotzky 2000; Grandi, Malaguti & Fiacchi 2006 for AGN and Fender, Belloni & Gallo 2004 for Galactic black holes). Explanations for these findings include highly ionized accretion discs (Ballantyne, Ross & Fabian 2002) and dilution by jet emission (e.g. Page et al. 2005), but the usually favoured interpretation is that the thin accretion disc in radio-loud objects is truncated at large radii and replaced by an advection-dominated accretion flow (ADAF). The latter explanation is especially appealing in terms of jet production, as ADAFs are thought to naturally lead to bipolar

outflows (Narayan & Yi 1994, 1995). While ADAFs are expected to exist within objects with very low accretion rates ($\dot{M}/\dot{M}_{\text{Edd}} \lesssim 0.01$, Rees et al. 1982), such as low-luminosity AGN and Galactic black holes in their low/hard states, they are unlikely to be present in radio-loud quasars, which generally have higher accretion rates.

Over the past few years there have been several reports of radio-loud objects, most of them quasars, where the presence of very broad Fe lines suggest that the accretion disc extends close or all the way in to the innermost stable orbit. Examples include the radio-loud AGN 4C +74.26 (Ballantyne & Fabian 2005), 3C 273 (Türler et al. 2006), PG 1425+267 (Miniutti & Fabian 2006), 3C 109 (Allen et al. 1997; Miniutti et al. 2006) and 3C 120 (Kataoka et al. 2007), as well as the Galactic black hole GX 339-4 in its low/hard state (Miller et al. 2006). These findings strongly indicate that a truncated thin disc is not a necessary condition for jet formation, and in particular not appropriate for objects with relatively high accretion rates. In this paper we will present the analysis of a new *Suzaku* observation of one of these objects, 4C +74.26.

4C +74.26 is a broad line radio galaxy (BLRG) located at $z = 0.104$ (Riley et al. 1989). Its radio luminosity is on the boarder of FR II and FR I but its morphology is clearly that of an FR II object (Riley et al. 1989). A one-sided jet which is at least 4 kpc long has been observed with the VLA (Riley & Warner 1990), and on parsec scales with VLBI (Pearson et al. 1992). Based on the flux-limit for a counter jet, Pearson et al. (1992) find that the inclination of the source axis must be

* E-mail: jlarsson@ast.cam.ac.uk

less than 49° to the line of sight. The bolometric luminosity of the source is around 2×10^{46} erg s^{-1} , making it a low-luminosity quasar (Woo & Urry 2002). The same authors also estimate a black hole mass of $4 \times 10^9 M_\odot$, which means that the source is operating at an Eddington ratio of ~ 0.04 .

4C +74.26 was first detected in the X-rays in the ROSAT All-Sky Survey, but the first observation that allowed a detailed spectral analysis was carried out with *ASCA* in 1996 (Brinkmann et al. 1998). Brinkmann et al. (1998) detected an Fe line with $EW \approx 100$ eV but could not determine if the line was broadened. The continuum could be well fitted with a model consisting of a power law and cold reflection (with a large reflection fraction of ~ 6), modified by absorption at low energies. The *ASCA* data were later re-analysed by Sambruna, Eracleous & Mushotzky (1999), who favoured a double power-law model for the continuum, in which the hard power law was attributed to emission from a jet. For the double power-law model the Fe line was found to be broad ($\sigma \sim 0.6$ keV) and the equivalent width higher (~ 200 eV).

The spectrum of a subsequent *BeppoSAX* observation could be described with a similar model as the one presented by Brinkmann et al. (1998), but with a significantly smaller reflection fraction of around 1 (Hasenkopf, Sambruna & Eracleous 2002). An *XMM-Newton* observation later revealed a broad Fe line, which implied an inner disc radius close to the innermost stable circular orbit for a maximally spinning black hole (Ballantyne & Fabian 2005). At low energies the *XMM-Newton* spectrum showed evidence for both cold and warm absorption (Ballantyne 2005). 4C +74.26 has also been detected in the *Swift* BAT and *INTEGRAL* surveys (Tueller et al. 2007 and Bodaghee et al. 2007, respectively).

In this paper we present the results of a 158 ks (~ 90 ks net exposure) *Suzaku* observation of 4C +74.26 performed in October 2007. We also carry out joint fits with the *XMM-Newton* observation performed in February 2004, and briefly discuss the data from the *Swift* BAT and *INTEGRAL* catalogs. Our main goal is to try and determine the inner radius of the accretion disc. This paper is organised as follows: Section 2 describes the observations and the data reduction, Section 3 describes the variability and Section 4 describes the spectral analysis. We finally discuss our results in Section 5 and present our conclusions in Section 6.

2 OBSERVATIONS AND DATA REDUCTION

4C +74.26 was observed by *Suzaku* between 2007 October 28–30 for a total duration of 158 ks. Event files from version 2.1.6.16 of the *Suzaku* pipeline processing were used and spectra were extracted using `XSELECT`.

For each XIS, source spectra were extracted from circular regions of 4.3 arcmin radius centred on the source (which was observed off-axis in the HXD nominal position). Background spectra were extracted from two circular regions with the same total area as the source region, avoiding the chip corners with the calibration sources. Response matrices and ancillary response files were generated for each XIS using `XISRMFGEN` version 2007-05-14 and `XISSIMARFGEN` version 2007-09-22. The ARF generator should account for the hydrocarbon contamination on the optical blocking filter (Ishisaki et al. 2007).

The net exposure time of all three XIS detectors is 92 ks and the 2–10 keV count rates are 0.753 ± 0.003 counts s^{-1} (XIS0), 0.806 ± 0.003 counts s^{-1} (XIS1) and 0.854 ± 0.003 counts s^{-1} (XIS3). Because of the very similar spectra of the two front-illuminated (FI) detectors (XIS0 and XIS3), their spectra were co-added for the spectral analysis, and their response files were combined accordingly.

For the HXD/PIN detector, a model for the non-X-ray background (NXB) was provided by the HXD team. Source and background spectra were constructed from identical good time intervals, and the exposure time of the background spectrum was increased by a factor of 10 (to account for the fact that the background model was generated with 10 times the actual count rate in order to minimize the photon noise). The source spectrum was corrected for dead time, leaving a total net exposure time of 86 ks. The response file appropriate for the HXD aim point was used (`ae_hxd_pinhxname4_20070914.rsp`).

The total PIN count rate over the 14–30 keV energy range is 0.3860 ± 0.0021 counts s^{-1} , compared to 0.2743 ± 0.0005 counts s^{-1} for the background. Since the background is so much brighter than the source, the accuracy of the background model is very important for our results. According to Mizuno et al. (2007), the one-sigma uncertainty of version 2 background models is around 3 per cent. It is often possible to determine the accuracy of the background model in a given observation more precisely by comparing it with the night earth spectrum. However, in the case of 4C +74.26 the PIN field of view was never completely obscured by the earth, and such a comparison is not possible. Some information on the accuracy of the background can also be obtained by comparing the light curves of the source and the background. This will be carried out in section 3.

The background model discussed above does not include the contribution from the cosmic X-ray background (CXB). In order to account for this we simulate the spectrum of the CXB and add it to the spectrum of the non-X-ray background. For the simulation of the CXB spectrum we use a model of the form $8 \times 10^{-4} (E/1 \text{ keV})^{-1.29} \exp(-E/40 \text{ keV})$, which is based on the HEAO-A1 spectrum, renormalized to the HXD field of view. The CXB count rate in the 14–30 keV band is about 6 per cent of the count rate of the total background (NXB + CXB).

2.1 The *XMM-Newton* observation

XMM-Newton observed 4C +74.26 on 2004 February 06 for a total duration of 34 ks. The data were reduced as described in Ballantyne (2005), using the *XMM-Newton* Science Analysis System version 7.1.0. We use only the data from the EPIC pn camera, which, after removing intervals of background flaring, has a total good exposure time of 29 ks.

3 VARIABILITY

3.1 light curves

Fig. 1 shows the 0.5–10 keV XIS light curve from the *Suzaku* observation of 4C +74.26. The light curve was obtained by adding the light curves of all three XIS detectors, using fully-exposed 1 ks bins. The source brightens by about

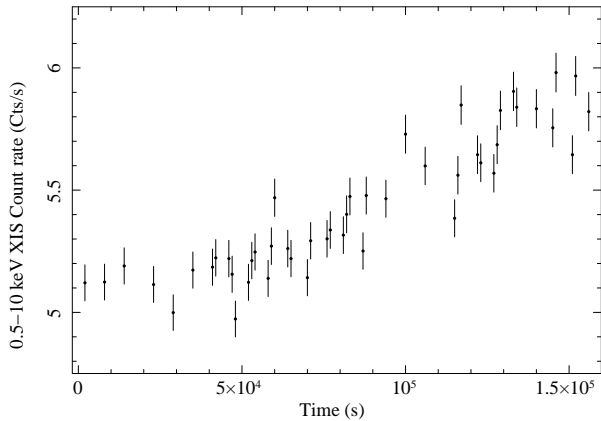


Figure 1. 0.5-10 keV XIS (0+1+3) light curve on a 1 ks time-scale, using only fully-exposed bins.

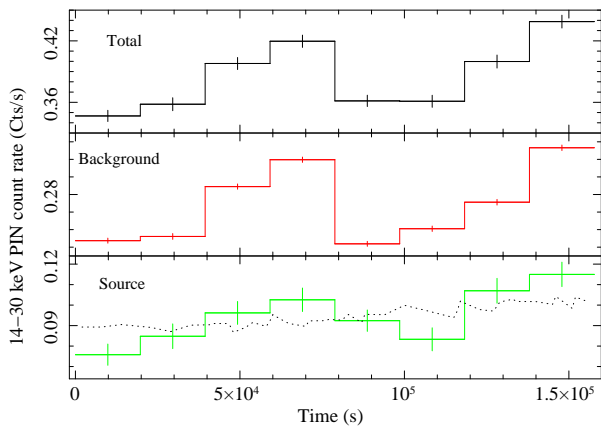


Figure 2. 14–30 keV PIN light curves on a 20 ks time-scale. Panels from top to bottom show the total light curve, the light curve of the NXB model, and the source light curve (where both the NXB model and the constant contribution from the CXB have been subtracted). As a reference the bottom panel also shows the XIS light curve (dotted line), rescaled to the mean PIN count rate. The background-subtracted light curve is clearly correlated with the background model, suggesting that the background has been underestimated.

20 per cent during the observation. We also note that the 2–10 keV flux has gradually increased by about a factor of two since the source was observed by *ASCA* in 1996, as summarized in Table 1. The flux in the soft band in the *ASCA* observation was also found to be two times higher than in a *ROSAT* observation in 1993 (when the source was in the field of view of an observation targeted at the cataclysmic variable VW Cep, Brinkmann et al. 1998). The 2–10 keV flux in the *Suzaku* observation is $3.24 \times 10^{-11} \text{ erg cm}^{-2} \text{ s}^{-1}$, corresponding to a luminosity of $8.80 \times 10^{44} \text{ erg s}^{-1}$.

In Fig 2 we show 14–30 keV PIN light curves on a 20 ks time-scale. Specifically, we compare the total light curve, the light curve of the NXB model, and the light curve of the source. The source light curve was obtained by subtracting both the NXB model and the constant contribution from the CXB. As a reference we also show the XIS light curve, rescaled to the mean PIN count rate. The light curves of the background model and the source are clearly correlated

Obs. date	Mission	2-10 keV flux ($10^{-11} \text{ erg cm}^{-2} \text{ s}^{-1}$)	Reference
2007-10-28	<i>Suzaku</i>	3.24	(1)
2004-02-06	<i>XMM-Newton</i>	2.43	(2)
1999-05-17	<i>BeppoSAX</i>	1.41	(3)
1996-09-09	<i>ASCA</i>	1.69	(4)

Table 1. 2–10 keV fluxes of *4C +74.26*. References: (1) This paper, (2) Ballantyne & Fabian (2005), (3) Hasenkopf et al. (2002), (4) Sambruna et al. (1999).

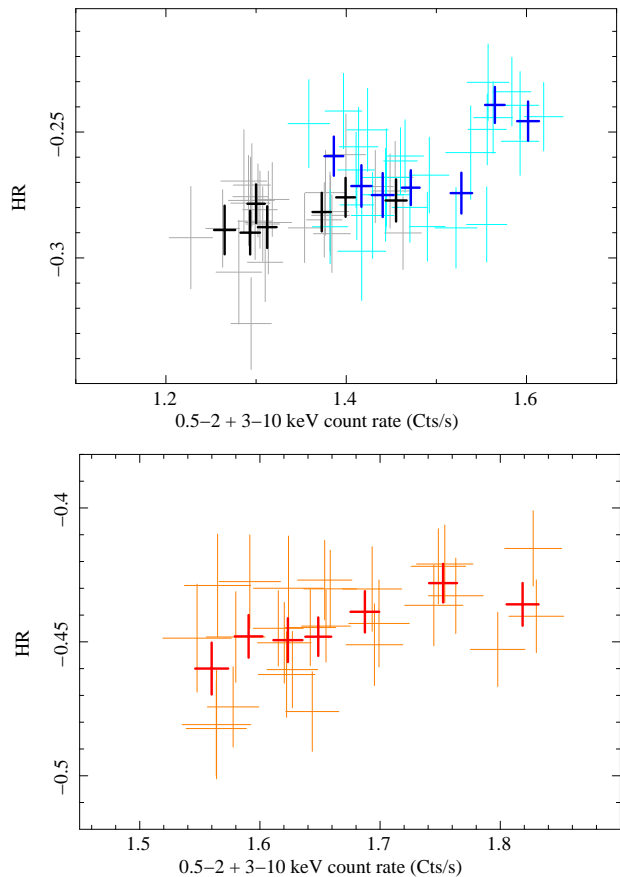


Figure 3. hardness ratios as a function of count rate for XIS 0 and 3 (black and blue crosses, upper panel) and XIS1 (lower panel). The hardness ratio is defined as $HR=(H-S)/(H+S)$, where S is the count rate in the 0.5 – 2 keV band and H is the count rate in the 3 – 10 keV band. The hardness ratios are calculated based on ~ 6 ks spectra. The thin crosses represent un-binned data points and the thick ones show the mean of data points binned along the x-axis. Each bin contains four original data points, apart from the last bin which contains three. For all three XIS we see that the spectrum tends to harden as the count rate increases.

(the cross-correlation function peaks at a value of 0.82 at 0 time lag), indicating that the background model has been underestimated.

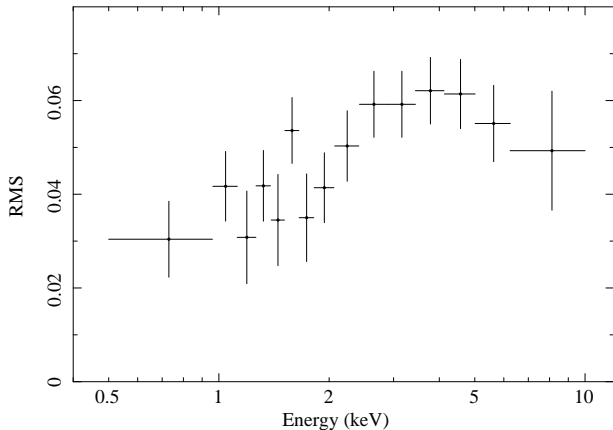


Figure 4. Rms spectrum of the entire observation calculated on the orbital time scale (~ 6 ks). The spectrum was calculated as an average of the rms spectra of the three XIS detectors.

3.2 Hardness ratios

In order to characterise the spectral variability of the source we start by calculating hardness ratios, $HR = H - S / H + S$, where we take H to be the count rate in the 3–10 keV band and S to be the count rate in the 0.5–2 keV band. The hardness ratios for all three XIS, calculated in orbital length bins of 5760 s, are plotted as a function of the $H + S$ count rate in Fig. 3. In order to reduce the scatter in the plot we binned consecutive points along the x-axis so that each bin comprises four original data points (apart from the last bin which contains three data points). Un-binned and binned data are shown as thin and thick crosses, respectively.

For all three XIS we see that the spectrum tends to harden as the count rate increases, although within a fairly large spread. In agreement with this, we find that a positive correlation is a better fit than a constant for all three data sets. According to an F-test, the improvement in the fit for un-binned (binned) data is significant at 91 (93) per cent (XIS0), 99 (99) per cent (XIS1) and 98 (87) per cent (XIS3). The fact that the positive correlation is highly significant only in XIS1 is presumably due to the higher effective area at low energies in this detector, which reduces the error on the count rate in the soft band.

3.3 The rms spectrum

We next consider the root-mean-squared (rms) spectrum, which, for a given time-scale, shows the fractional variability as a function of energy. The techniques for calculating rms spectra are described in e.g. Edelson et al. (2002) and Vaughan et al. (2003). Fig. 4 shows the rms spectrum of 4C +74.26, calculated as an average of the rms spectra of the three XIS detectors, on the orbital time-scale of 5760 s. The errors from the Poisson noise were calculated following Vaughan et al. (2003). The rms variability clearly increases with energy up to about 4 keV, at which point it flattens out and shows some evidence of decreasing.

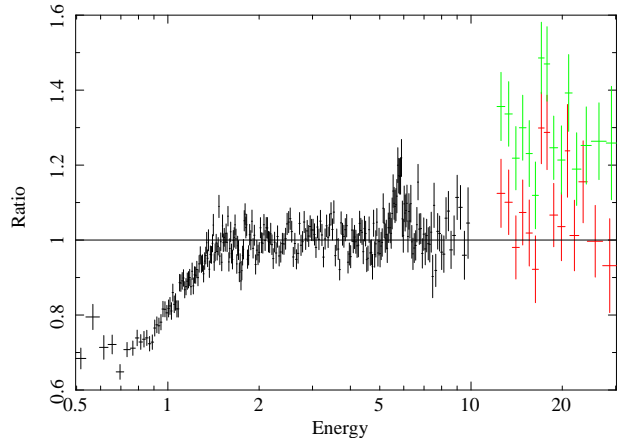


Figure 5. FI XIS + PIN spectrum as a ratio to a power law (modified by Galactic absorption), fitted over the 2–4 and 7–10 keV energy ranges. The red and green data points show the PIN data assuming a background model of ± 3 per cent (the one-sigma accuracy of v2 background models). The study of the PIN light curves in section 3.1 showed that the background has probably been underestimated, suggesting that the real value should be closer to the red data points. The low-energy data clearly reveal the presence of absorption in excess of the Galactic value.

4 SPECTRAL ANALYSIS

In the spectral analysis of the *Suzaku* data we will concentrate on the 2–10 keV (XIS) and 14–30 keV (PIN) energy ranges. We find that the agreement between the FI XIS is very good in the 2–10 keV range, and we therefore add their spectra, as previously mentioned in section 2 and recommended in the *Suzaku* Data Reduction Guide. The spectrum of XIS1, on the other hand, differs significantly from the FI XIS spectra in the Fe $K\alpha$ region (the line energy and width are inconsistent with the FI XIS values), and we do not include it in our spectral analysis. Because of inconsistencies between the XIS detectors at low energies (presumably due to the modelling of the contamination), we do not extend the spectral analysis below 2 keV at this time. We note, however, that the low-energy spectrum is characterized by absorption in excess of the Galactic value (see Fig. 5), in agreement with previous observations. The absorption is not strong enough to affect the spectrum above 2 keV.

Below we will first consider the 2–10 keV FI XIS spectrum and then include the high-energy PIN data. We will also investigate the high-energy properties of the source using the spectra from *Swift* and *INTEGRAL*. As a last step we will perform joint fits to the *Suzaku* and *XMM-Newton* 2–10 keV spectra. All spectral fits were performed using XSPEC version 11.3.2aj. Errors on model parameters are quoted at the 90 per cent confidence level and energies of spectral features are quoted for the rest frame of the source. All fits include Galactic absorption fixed at $N_H = 1.19 \times 10^{21} \text{ cm}^{-2}$ (Dickey & Lockman 1990).

4.1 The 2–10 keV FI XIS spectrum

In order to look for the presence of a broad Fe line we start by fitting the spectrum with a power law, excluding the 4–7 keV energy band, where the line emission should dominate.

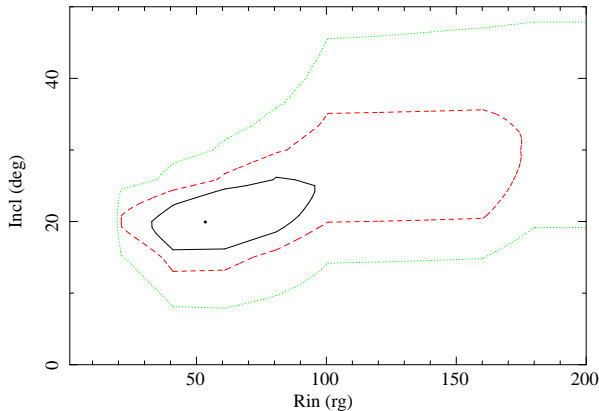


Figure 6. Confidence contours for r_{in} and i in the model consisting of a power law and a Laor line. The black (solid), red (dashed) and green (dotted) lines represent 1, 2 and 3 sigma confidence, respectively. The best fit is shown as a black dot.

Fig. 5 shows the data as a ratio to the power-law fit (which has $\Gamma = 1.81 \pm 0.01$), clearly revealing that a broadened line is present. The fact that the line is broadened is confirmed when we add a Gaussian line to the power-law model. If we let the width of the line be a free parameter we find an excellent fit of $\chi^2 = 1510$ for 1509 degrees of freedom (d.o.f.), compared to $\chi^2/\text{d.o.f.} = 1546/1510$ if we force the line to be narrow ($\sigma = 1$ eV). The broad line has $\sigma = 0.24_{-0.07}^{+0.08}$ keV and $EW = 85_{-19}^{+20}$ eV. The results of these fits as well as all other spectral fits discussed in this section are presented in Table 2.

Broad Fe lines are often found to have a narrow component originating from distant matter. To check for such a component in 4C +74.26 we add a narrow line at 6.4 keV to the model with the broad Gaussian. This improves the fit by only $\Delta\chi^2 = -2$ for 2 fewer degrees of freedom, and the narrow line is found to have a very low equivalent width of 10_{-10}^{+15} eV. We thus conclude that a narrow component to the Fe line is not required.

We next replace the broad Gaussian with a Laor line (Laor 1991), which models the Fe line emission from an accretion disc around a Kerr black hole. We fix the energy of the line at 6.4 keV, the outer radius of the disc at $r_{\text{out}} = 400 r_g$ (where $r_g = GM/c^2$ is the gravitational radius), and the emissivity index of the disc at $q = 3$ (the emissivity follows the form $\epsilon \propto r^{-q}$, where r is the radius of emission, and $q = 3$ is expected from gravitational energy release). This leaves the inner radius of emission (r_{in}), the inclination of the disc (i) and the normalization of the line as free parameters. We find an excellent fit of $\chi^2/\text{d.o.f.} = 1514/1509$ with $r_{\text{in}} = 53_{-28}^{+119} r_g$ and $i = 20_{-5}^{+8^\circ}$.

The relatively low inclination obtained in this fit implies that the source is extremely large (of the order of 3 Mpc). This is still smaller than the largest radio galaxy observed to date (3C 236 is ~ 4.5 Mpc, Saripalli & Mack 2007) but larger than the majority of the known radio galaxies. Assuming that the size of 4C +74.26 is around 2 Mpc, which is more typical for a giant radio galaxy, the inclination should be around 33° . If we fix the inclination at this value we obtain a fit which is only slightly worse ($\chi^2/\text{d.o.f.} = 1518/1510$), but which has a significantly larger r_{in} of $177_{-77}^{+223} r_g$. The relationship between the inclination and r_{in} can be seen in

Fig. 6, which shows the confidence contours for these parameters in the fit where the inclination was left free. We note that the three-sigma confidence contour remains below 50° , in agreement with the upper limit on the inclination of 49° set by Doppler boosting arguments (Pearson et al. 1992).

The relatively large values obtained for r_{in} in the fits described above suggest that the inner disc in 4C +74.26 is either not present or for some reason unable to produce strong fluorescent Fe emission. In order to check if a fit where the Fe emission is produced in the inner regions of the disc can be obtained, we refit the data with r_{in} fixed at $1.24 r_g$ (the innermost stable circular orbit of a Kerr black hole). We find that a narrow 6.4 keV line has to be added to the model in order to obtain an acceptable fit for this scenario. The quality of the fit is worse than for the case of a free r_{in} ($\Delta\chi^2 = +15$ for one less d.o.f) but we note that the combination of the small r_{in} and the narrow line results in a higher inclination of $40_{-6}^{+4^\circ}$.

In order to also model the reflection spectrum associated with the Fe line, we next replace the Laor line with the REFLION model by Ross & Fabian (2005), which models the emission from a constant-density accretion disc. The parameters of the model are the Fe abundance, the ionization parameter ξ , the photon index of the incident power law and the normalization. In order to account for the relativistic effects in the vicinity of the black hole, the reflection model is convolved with the relativistic blurring kernel `KD-BLUR`, which is derived from the code by Laor (1991) (the model parameters are the inner and outer radius of the disc, the inclination and the emissivity index). We leave all parameters free to vary apart from the outer radius of the disc and the emissivity index, which we fix at $r_{\text{out}} = 400 r_g$ and $q = 3$, respectively.

We find a best fit of $\chi^2/\text{d.o.f.} = 1514/1506$ with $r_{\text{in}} = 68_{-25}^{+332} r_g$ and $i = 21_{-6}^{+18^\circ}$, which is very similar to our best-fitting Laor model. As in the case of the Laor model, the fit only becomes slightly worse if the inclination is fixed at a larger value. We are also still able to obtain an acceptable fit with r_{in} fixed at $1.24 r_g$ if a narrow line at 6.4 keV is included. As before, this fit is somewhat worse ($\Delta\chi^2 = +13$ for one less d.o.f) and has a higher inclination ($42_{-5}^{+4^\circ}$). In both reflection fits the ionization parameter of the disk is 30 erg cm s^{-1} , i.e. nearly neutral, and the Fe abundance is about 2 times solar. Both models are plotted in Fig. 7 together with the fit residuals. It is clear that the first model (with the larger r_{in} and lower inclination) is a better fit in the Fe line region. We also note the presence of a narrow feature around 7.2–7.4 keV (6.5–6.7 keV in the observed frame). We will discuss the possible origin of this feature in section 4.1.1 below.

In addition to the interpretation that the inner disc is missing, there are several possible scenarios that could explain the large values obtained for r_{in} in our best-fitting models. For example, extreme ionization of the inner disc would lead to a nearly featureless reflection spectrum that would be hard to disentangle from the power law continuum. In fact, adding an inner reflector with ξ fixed at $10^4 \text{ erg cm s}^{-1}$ (the highest allowed value) to our best-fitting reflection model results in an acceptable fit, although the quality of the data is not good enough to constrain the fit parameters.

Another possible reason for the large value of r_{in} is that

Model	Γ	$E_{G/L}$	σ_G	$EW_{G/L}$	E_{nl}	EW_{nl}	r_{in}	i	Fe	ξ	χ^2/dof
pl + nl	$1.80^{+0.01}_{-0.01}$				$6.40^{+0.05}_{-0.04}$	31^{+8}_{-8}					1546/1510
pl + G	$1.82^{+0.01}_{-0.02}$	$6.38^{+0.06}_{-0.05}$	$0.24^{+0.08}_{-0.07}$	85^{+20}_{-19}							1510/1509
pl + G + nl	$1.82^{+0.01}_{-0.01}$	$6.38^{+0.09}_{-0.09}$	$0.30^{+0.12}_{-0.10}$	78^{+28}_{-23}	$6.42^{+0.09}_{-0.10}$	10^{+15}_{-10}					1508/1507
pl + Laor	$1.81^{+0.01}_{-0.01}$	6.40^f		70^{+13}_{-16}			53^{+119}_{-28}	20^{+8}_{-5}			1514/1509
pl + Laor + nl	$1.82^{+0.01}_{-0.01}$	6.40^f		116^{+51}_{-51}	$6.40^{+0.05}_{-0.05}$	25^{+8}_{-9}	1.24^f	40^{+4}_{-6}			1530/1508
pl + blr*ref	$1.84^{+0.03}_{-0.03}$						68^{+332}_{-25}	21^{+18}_{-6}	$1.8^{+8.2}_{-0.8}$	30^{+34}	1514/1506
pl + blr*ref + nl	$1.87^{+0.05}_{-0.04}$				$6.40^{+0.05}_{-0.05}$	27^{+9}_{-10}	1.24^f	42^{+4}_{-5}	$1.6^{+1.0}_{-0.6}$	30^{+4}	1528/1507

Table 2. Fits to the 2–10 keV *Suzaku* FI XIS spectrum. The model components are pl = power law, nl = narrow Gaussian emission line (σ fixed at 1 eV), G = Gaussian emission line, Laor = Laor model, blr = KDBLUR (relativistic blurring kernel), ref = REFLION (reflection model). Γ is the photon index of the power law, $E_{G/L}$ is the energy of the broad Gaussian or Laor line (in keV), σ_G is the width of the Gaussian line (in keV), $EW_{G/L}$ is the equivalent width of the broad Gaussian or Laor line (in eV), E_{nl} is the energy of the narrow line (in keV), EW_{nl} is the equivalent width of the narrow line (in eV), r_{in} is the inner radius of the disc (in gravitational radii), i is the inclination of the disc to the line of sight (in degrees), Fe is the iron abundance of the disc (relative to solar), ξ is the ionization parameter of the disc (in $\text{erg cm}^{-2} \text{s}^{-1}$). Superscript f indicates that the parameter was frozen. The following parameters were always fixed: σ of the narrow line (1 eV), the outer radius of the disc (400 gravitational radii), the emissivity index of the disc (3). All fits also included absorption fixed at the Galactic value.

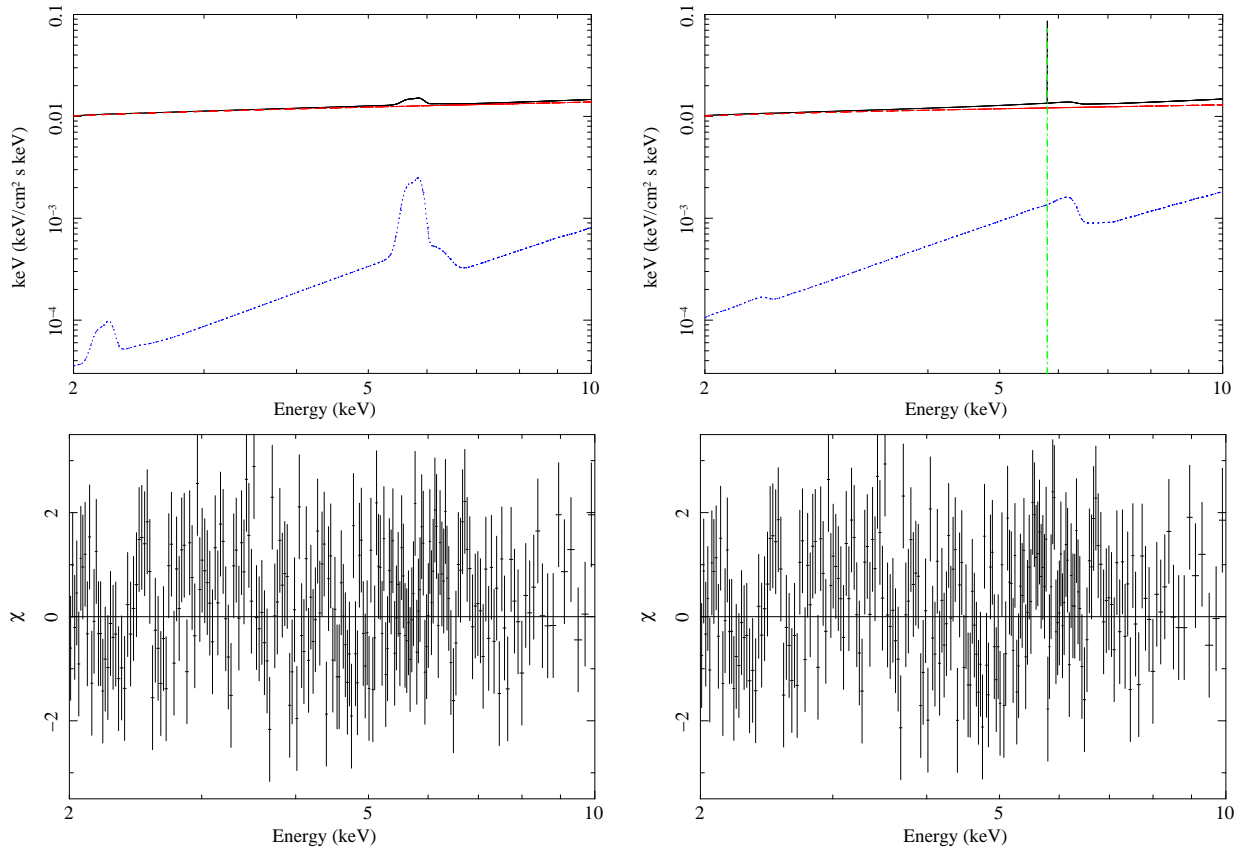


Figure 7. Reflection fits to the 2–10 keV *Suzaku* FI XIS spectrum. The top panel shows the best-fitting models together with their components, and the bottom panel shows the residuals to the fit. The model in the left panel consists of a power law and reflection from a disc truncated around $70 r_g$. The model shown in the right panel consists of a power law, reflection from a disc that extends all the way in to $1.24 r_g$, and a narrow Fe $K\alpha$ line. Black (solid) lines represent the total model, red (dashed) lines the power law, blue (dotted) lines the reflection model, and the green (dashed-dotted) line the narrow line.

the illumination of the disc results in an emissivity index that deviates from our assumed value of $q = 3$. The quality of the data does not allow us to constrain this parameter if all other parameters are left free. However, when fixing the other reflection parameters at their time-averaged values, we find that the model with $r_{\text{in}} = 1.24 r_{\text{g}}$ improves significantly with a flatter emissivity of $q \sim 1$. Such a flat emissivity would be expected (at least in an average sense) if the disc is illuminated from a great height ($\gtrsim 30 r_{\text{g}}$) in a lamp post geometry (see also Vaughan et al. 2004), or if the power-law emission originates in the base of a jet, which is beamed away from the inner disc.

A contribution from a jet in 4C +74.26 has previously been suggested for the *ASCA* observation of the source (Sambruna et al. 1999). In order to model this scenario we add a second, hard power law to the reflection models described above. The results of this are inconclusive though, as we find that we cannot obtain any meaningful constraints on the slope and normalization of the second power law.

4.1.1 The narrow feature around 7.4 keV

As mentioned above, the residuals in Fig. 7 reveal a narrow feature around 7.2–7.4 keV (6.5–6.7 keV in the observed frame). Depending on the underlying model, this feature can be modelled either as a 7.40 keV emission line or as a 7.17 keV absorption line.

For the model consisting of a power law and a broad Gaussian, the best fit is obtained with a narrow emission line at 7.40 keV (the fit improves by $\Delta\chi^2 = -8$ for 2 fewer degrees of freedom when the line is added, and $\text{EW} = 16 \pm 11$ eV). The same is true for the Laor and reflection models in table 2 that have r_{in} as a free parameter. None of the best-fitting parameter values change significantly when the line is added to these models. An absorption line at 7.17 keV results in a very small improvement of the fit for these models, and we especially note that the addition of the line does not significantly affect the inclination. This is also true if the absorption line is identified with Fe xxvi at 6.97 keV and we add a Fe xxv line (rest energy 6.7 keV) with the same blueshift.

For the models where $r_{\text{in}} = 1.24 r_{\text{g}}$ and a narrow 6.4 keV line is included, we find that the narrow feature can be equally well fitted with a 7.17 keV absorption line as with a 7.40 keV emission line. Specifically, in the case of the model which consists of a power law, a Laor line and a 6.4 keV line, we find that the absorption line improves the fit by $\Delta\chi^2 = -13$ for 2 fewer degrees of freedom and has $\text{EW} = 22_{-9}^{+10}$ eV, while the emission line results in $\Delta\chi^2 = -14$ for 2 fewer degrees of freedom and has $\text{EW} = 16_{-11}^{+10}$ eV. No model that includes both an absorption and an emission line can be found. Although the absorption line is an equally good fit as the emission line in this case, we note that the inclination goes up to about 55° when the absorption line is added. This is higher than the upper limit of 49° placed by Doppler boosting arguments (Pearson et al. 1992).

We have ruled out an instrumental origin for the lines, which suggests that they (if real) are due to highly blueshifted Fe emission. For example, identification of the 7.17 keV absorption line with Fe xxv at 6.70 keV would imply an outflow velocity of about $20\,000 \text{ km s}^{-1}$. This extreme

velocity together with the relatively low significance of the lines suggests that they are probably not real. However, it is interesting to note that Robinson et al. (1999) detected a redshifted H α line in polarised light in this source, indicating that an outflow with a velocity greater than $5\,000 \text{ km s}^{-1}$ is present.

4.2 The high-energy PIN spectrum

4C +74.26 is clearly detected in the PIN up to about 30 keV and we stress that this detection is robust against uncertainties in the background model. When fitting the data we use the model for the non-X-ray background provided by the HXD-team, and we account for the contribution from the CXB as described in section 2. The cross normalization of the PIN with respect to XIS0 has been reported to be about 1.14 for the HXD nominal position and v2 data (Ishida, Suzuki & Someya 2007). After adjusting this value for the difference in normalization between XIS0 and our added FI XIS spectrum, we adopt a PIN/FI XIS cross normalization of 1.12.

Fig. 5 shows the PIN + FI XIS spectrum as a ratio to a power law, fitted over the 2–4 and 7–10 keV energy ranges. In order to illustrate the uncertainties in the PIN data we show the spectra obtained by increasing and decreasing the background model by 3 per cent (the one-sigma uncertainty of v2 background models). We note that the study of the PIN light curves in section 3.1 showed that the background has probably been underestimated, suggesting that the real value is closer to the lower (red) data points. This also agrees with the predictions of the reflection models that were found to fit the 2–10 keV data. For the model where r_{in} is a free parameter we get a best 2–30 keV fit of $\chi^2/\text{d.o.f.} = 1561/1549$ if the background is increased by 2 per cent. Similarly, for the model with $r_{\text{in}} = 1.24 r_{\text{g}}$, we get a best chi-squared of $\chi^2/\text{d.o.f.} = 1573/1548$ if the background is increased by 1–2 per cent.

The relative contribution from the reflection component is usually measured by the reflection fraction, which is the ratio of the total reflected emission to the power-law emission. For an isotropic source illuminating an infinite plane of gas the reflection fraction is 1. We estimate the reflection fraction of our models by measuring the the unabsorbed fluxes in the two components within *XSPEC*. For the two models presented above the reflection fractions are 0.3 and 0.5, respectively, assuming that the power law emission extends all the way up to the upper boundary for the *REFLION* model. On the other hand, assuming an upper cutoff for the power law of 150 keV (as previously found for *BeppoSAX* data, Grandi et al. 2006) we find slightly higher reflection fractions of 0.4 and 0.7. In either case, it is clear that the reflection fraction is less than 1, implying e.g. that the illumination is anisotropic, that the disc is truncated or that an unreflected component (such as a jet) contributes to the spectrum.

4.3 Comparison with the Swift and INTEGRAL data

4C +74.26 is included in both the *Swift* BAT 9-month AGN catalog (Tueller et al. 2007) and the *INTEGRAL* general

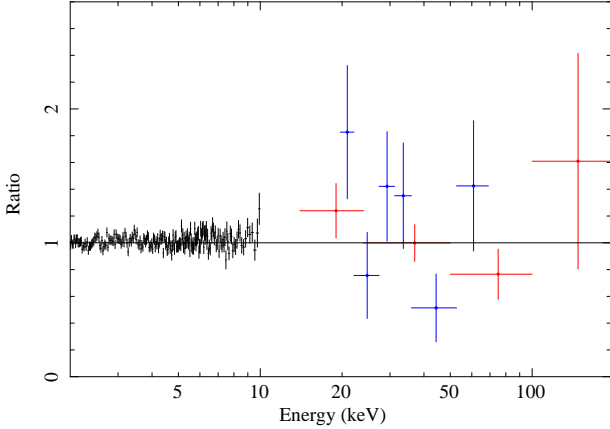


Figure 8. The *Suzaku* FI XIS spectrum (in black), together with the *Swift* (red) and *INTEGRAL* (blue) spectra, shown as a ratio to the best-fitting 2–10 keV reflection model. The normalizations of the *Swift* and *INTEGRAL* data were allowed to vary freely with respect to the XIS spectrum.

reference catalog (Bodhagee et al. 2007). In order to further investigate the high-energy properties of 4C +74.26 we briefly investigate the spectra from these catalogs in this section. The data from the BAT catalog are publicly available¹ and the *INTEGRAL* spectrum was provided by the *INTEGRAL* AGN team (the *INTEGRAL* data is also analysed in Molina et al. 2008, in prep).

A simple power-law fit to the data yields $\Gamma = 2.1^{+0.4}_{-0.3}$ for *Swift* (14–195 keV) and $\Gamma = 2.2^{+0.7}_{-0.6}$ for *INTEGRAL* (20–100 keV). This should be compared with $\Gamma = 1.8 \pm 0.2$ in the 14–30 keV range for the *Suzaku* PIN detector. No clear evidence for a cutoff of the power law is seen in any of the spectra. Based on the power-law fits the inferred 14–30 keV fluxes are $F_{14-30} = 1.4 \times 10^{-11}$ erg cm⁻² s⁻¹ (*Swift*) $F_{14-30} = 2.6 \times 10^{-11}$ erg cm⁻² s⁻¹ (*INTEGRAL*) and $F_{14-30} = 2.7 \times 10^{-11}$ erg cm⁻² s⁻¹ (*Suzaku* PIN). As the observations are not simultaneous and the source appears to be getting brighter (as shown in Table 1), it is not surprising that the photon indices and fluxes differ somewhat.

In order to check if the *Swift* and *INTEGRAL* data are consistent with a reflection model, we fit them with our best-fitting 2–10 keV reflection model, leaving only the cross-normalizations between the detectors as free parameter. As shown in Fig. 8, the shape of the high-energy spectra can be well reproduced by the reflection model ($\chi^2/\text{dof} = 1527/1524$ over the entire 2–195 keV range). The cross-normalizations with respect to the FI XIS are found to be 0.6 for *Swift* and 0.9 for *INTEGRAL*. We also note that the high-energy data can be equally well described with the reflection model with $r_{\text{in}} = 1.24 r_g$.

4.4 Fits including the previous *XMM-Newton* data

Fig. 9 shows a comparison of the *Suzaku* FI XIS spectrum and the EPIC pn spectrum from the previous *XMM-Newton* observation of 4C +74.26 (Ballantyne & Fabian

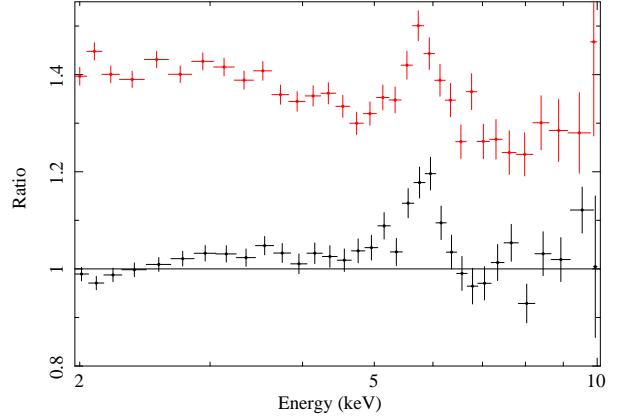


Figure 9. Comparison of the *XMM-Newton* EPIC pn (black) and *Suzaku* FI XIS (red) spectra. The plot shows the spectra as a ratio to a power law fitted to the *XMM-Newton* data, excluding the 4–7 keV energy band.

2005). The spectra are shown as a ratio to a power-law fitted to the *XMM-Newton* data, excluding the 4–7 keV energy range. It is clear from the plot that the continuum is somewhat steeper in the *Suzaku* observation ($\Delta\Gamma \sim 0.1$), while the Fe line profiles are very similar in both spectra.

In order to try and find a spectral model for both observations we performed simultaneous fits to the spectra, using the two different reflection fits obtained for the *Suzaku* data as a starting point. Experimentation showed that very good joint fits could be obtained for both models if all parameters apart from the slope and the normalization of the power law were tied between the two spectra. The results of the fits are presented in Table 3. We see that the model where r_{in} is a free parameter is still a somewhat better fit than the model with $r_{\text{in}} = 1.24 r_g$ ($\chi^2/\text{d.o.f.} = 2410/2538$ compared to 2431/2537). In both models the photon index of the power law is 0.1 steeper for *Suzaku* than for *XMM-Newton*. The only tied parameters that differ significantly from the values obtained when fitting only the *Suzaku* data are r_{in} , i and Fe of the first model. The values of these parameters have all increased (especially note that the inclination now has a more reasonable value of $31^{+12}_{-11}^\circ$) but they are all still consistent (within the errors) with the *Suzaku* fits. As in the case of the *Suzaku* fits, we also find that both models agree well with the high-energy PIN data, and that the best agreement is found if we assume that the background model has been underestimated by 2–3 per cent.

We stress that the reflection normalization is tied in these fits and that letting it vary independently for the two spectra does not improve the quality of the fits. The same is true for the normalization of the narrow 6.4 keV line. We thus conclude that the difference between the *Suzaku* and *XMM-Newton* observations can be well described in terms of a power law that has increased in normalization and also become slightly steeper.

As a final comment we note that there is evidence for a narrow 6.2 keV line in the *XMM-Newton* spectrum (EW ~ 20 eV, as previously noted by Ballantyne & Fabian 2005) but not in the *Suzaku* spectrum. The origin of this line is unclear but Ballantyne & Fabian (2005) suggested that it

¹ <http://swift.gsfc.nasa.gov/docs/swift/results/bs9mon/>

Model	Γ_s	Γ_x	r_{in}	i	Fe	ξ	E_{nl}	$\text{EW}_{\text{nl},s}$	$\text{EW}_{\text{nl},x}$	χ^2/dof
pl + blr*ref	$1.83^{+0.02}_{-0.02}$	$1.72^{+0.01}_{-0.02}$	161^{+239}_{-117}	31^{+12}_{-11}	$3.8^{+6.2}_{-2.2}$	30^{+21}				2410/2538
pl + blr*ref + nl	$1.86^{+0.03}_{-0.04}$	$1.76^{+0.05}_{-0.05}$	1.24^{f}	40^{+4}_{-5}	$2.5^{+7.5}_{-0.8}$	30^{+9}	$6.4^{+0.04}_{-0.02}$	28^{+7}_{-8}	36^{+10}_{-10}	2431/2537

Table 3. Combined 2–10 keV reflection fits to the *Suzaku* and *XMM-Newton* spectra. The model components are pl = power law, blr = KDBLUR (relativistic blurring), ref = REFLION (reflection model), nl = narrow Gaussian emission line (σ fixed at 1 eV). Γ is the photon index of the power law, r_{in} is the inner radius of the disc (in gravitational radii), i is the inclination of the disc to the line of sight (in degrees), Fe is the iron abundance of the disc (relative to solar), ξ is the ionization parameter of the disc (in $\text{erg cm}^{-2} \text{s}^{-1}$), E_{nl} is the energy of the narrow line (in keV), EW_{nl} is the equivalent width of the narrow line (in eV). Subscripts s and x denote values for the *Suzaku* and *XMM-Newton* spectra, respectively. All parameters were tied between the two spectra apart from the photon index and the normalization of the power law. Superscript f indicates that the parameter was frozen. The following parameters were fixed in all the fits: the outer radius of the disc (400 gravitational radii), the emissivity index of the disc (3), σ of the narrow line (1 eV). All fits also included absorption fixed at the Galactic value.

and the 6.4 keV line could form the red and blue horns of a diskline originating in the outer disc.

5 DISCUSSION

5.1 Spectral variability

Due to the long duration of the *Suzaku* observation, we have for the first time detected variability in the light curve of 4C +74.26. We find that the source brightens by about 20 per cent during the observation, implying a doubling time of ~ 1 Ms. There is evidence for a positive correlation between the hardness ratio and the count rate, although this is only significant at the 99 per cent level in the case of XIS1. We also find that the rms variability increases with energy up to about 4 keV, at which point it flattens out and shows evidence of decreasing. This spectral variability is rather different from that observed in typical radio-quiet Seyfert galaxies, which generally exhibit spectral softening with increasing count rate and rms variability decreasing with energy above ~ 1 keV (e.g. Papadakis et al. 2002; Markowitz & Edelson 2004).

One possible explanation for the spectral variability observed in 4C +74.26 is that a jet contributes to the spectrum. This is possible even if the inclination of the jet to the line of sight is fairly large, as the base of the jet may not be well collimated. In this picture, our measured photon index of ~ 1.8 would be due the combined contributions from a hard component associated with the jet, and a softer component associated with Comptonized emission from the corona, as previously suggested for an *ASCA* observation of the source (Sambruna et al. 1999). The fact that the source is harder when it is brighter would then indicate that the relative contribution from the jet is higher when the flux increases, assuming that the intrinsic slopes of the two power laws do not vary significantly. Such a model could in principle be tested by investigating the difference spectrum between high- and low-flux spectra. However, due to the limited amplitude of the variability in 4C +74.26 we find that the difference spectrum is not of sufficient quality to discriminate between models.

5.2 Spectral modelling

In our spectral analysis of the *Suzaku* data of 4C +74.26 we clearly detect a broad Fe line, as previously seen by *XMM-Newton* (Ballantyne & Fabian 2005). Our best fits to the Fe line profile suggest that the line originates outside about $50 r_g$ and that the inclination to the line of sight is around 20° . This inclination implies that the source is around 3 Mpc across, which is extremely large even for a giant radio galaxy. Although it is possible that the source actually is this large, we note that an almost equally good fit can be obtained if the inclination is fixed at a larger value. For this scenario the inner radius of emission is outside $100 r_g$. We also managed to find a good fit with a model in which r_{in} was fixed at $1.24 r_g$. This model has the advantage of a higher inclination of around 40° , but is a worse fit in the Fe line region and also relies on the presence of a narrow Fe K α line, which is not required in any other model. Overall it seems like the first model is a better approximation of the real conditions.

The perhaps simplest explanation for these findings is that the inner accretion disc is missing, as suggested for many other radio-loud AGN (e.g. Eracleous et al. 2000). It is also possible, however, that the inner disc is highly ionized or not strongly illuminated. The latter explanation seems more likely, as the former model would require a very sharp transition from an extremely ionized to a nearly neutral disc. A plausible explanation for why the inner disc is not strongly illuminated is that the corona, where the power law originates, is located high above the disc.

The coronae of AGN are widely believed to be powered by magnetic fields in their accretion discs. As magnetic fields are thought to be important for jet formation (e.g. Blandford & Payne 1982), it is likely that the properties and structure of the magnetic fields in radio-quiet and radio-loud objects are different. The strong reflection features often seen in radio-quiet AGN indicate that their inner discs are strongly illuminated, implying that the magnetic energy is dissipated close to the disc. It is conceivable that the magnetic field structure in radio-loud objects leads to the energy being dissipated at larger heights, possibly in a region moving away from the disc, thus resulting in less illumination of the inner disc and weaker reflection features.

It is also possible that emission from the jet itself contributes to the spectrum, as tentatively suggested by the variability properties described above. We explicitly tested for the presence of a jet in the *Suzaku* spectrum by adding a

second, hard power law to the power law + reflection model. The results were inconclusive, however, as we found that we could not constrain the properties of the second power law. A much longer observation would be needed to put constraints on the possible jet component in 4C +74.26.

The difference between the 2007 *Suzaku* and 2004 *XMM-Newton* spectra can be well modelled with a power law that has increased in normalization and become slightly steeper. The reflected emission is consistent with staying constant between the observations, and the best-fitting disc parameters in the joint fits are similar to those found when only fitting the *Suzaku* data. A possible explanation for this behaviour is that the increase in flux between the two observation is mainly due to the (unreflected) emission from the jet increasing, in combination with the slope of the coronal and/or jet power laws steepening somewhat.

6 SUMMARY AND CONCLUSIONS

We have analysed a 92 ks exposure *Suzaku* observation of the radio quasar 4C +74.26. Our main results can be summarized as follows:

- The 2–10 keV flux measured by *Suzaku* is 3.24×10^{-11} erg cm⁻² s⁻¹, which is the highest flux observed to date. The source has gradually brightened by about a factor of two since it was first observed by *ASCA* in 1996.

- Due to the long observation, we have for the first time detected variability in the light curve of 4C +74.26. We find that the count rate increases by about 20 per cent during the observation.

- There is evidence for spectral hardening as the count rate of the source increases. We also find that rms variability increases with energy up to about 4 keV, where it flattens out and shows some evidence of decreasing.

- We clearly detect a broadened Fe K α line. When fitted with a simple Gaussian, it has $EW = 85$ eV and $\sigma = 0.24$ keV.

- The entire 2–30 keV energy range can be well fitted with a power law ($\Gamma \approx 1.8$) and near-neutral reflection from an accretion disc. No reflected emission inside about $50 r_g$ is required by the Fe line profile, although a model with $r_{in} = 1.24 r_g$ provides a good fit if a narrow Fe K α line is included. The reflection fraction is found to be in the range ~ 0.3 – 0.7 , depending on the model.

- The high-energy *Swift* BAT and *INTEGRAL* spectra show a somewhat steeper continuum slope ($= \Gamma \sim 2.1$ – 2.2) but can nevertheless be well described with the power-law + reflection models described above.

- The difference between the *Suzaku* and *XMM-Newton* 2–10 keV spectra can be well explained with a power law that has increased in normalization and become slightly steeper.

The spectral variability properties described above can be explained in a model where the relative contribution from a hard jet increases with increasing flux. However, because of the limited variability amplitude and spectral quality, we are not able to constrain the possible contribution from a jet in 4C +74.26. The best-fitting reflection model implies that the inner disc is either truncated at large radii or not strongly illuminated. We suggest that the latter scenario may be due to the power-law source being located high above the disc, e.g. as a result of the magnetic field structure.

7 ACKNOWLEDGEMENTS

We thank Alessandra De Rosa for providing the *INTEGRAL* spectrum. JL thanks Corpus Christi College, the Isaac Newton Trust and STFC. ACF thanks the Royal Society for support. D. R. B. is supported by the University of Arizona Theoretical Astrophysics Program Prize Postdoctoral Fellowship.

REFERENCES

- Allen S. W., Fabian A. C., Idesawa E., Inoue H., Kii T., Otani C., 1997, MNRAS, 286, 765
 Ballantyne, D.R., Ross, R.R. & Fabian, A.C., 2002, MNRAS, 332, L45
 Ballantyne D. R., 2005, MNRAS, 362, 1183
 Ballantyne D. R., Fabian A. C., 2005, ApJ, 622, L97
 Ballantyne D. R., 2007, MPLA, 22, 2397
 Blandford R. D., Payne D. G., 1982, MNRAS, 199, 883
 Bodaghee A., et al., 2007, A&A, 467, 585
 Brinkmann W., Otani C., Wagner S. J., Siebert J., 1998, A&A, 330, 67
 Dickey J. M., Lockman F. J., 1990, A&A, 28, 215
 Edelson R., Turner T. J., Pounds K. Vaughan S., Markowitz A., Marshall H., Dobbie P., Warwick R., 2002, ApJ, 568, 610
 Eracleous M., Sambruna R. M., Mushotzky R. F., 2000, ApJ, 537, 654
 Fender R. P., Belloni T. M., Gallo E., 2004, MNRAS, 355, 1105
 Grandi P., Malaguti G., Fiacchi M., 2006, ApJ, 642, 113
 Hasenkopf C. A., Sambruna R. M., Eracleous M., 2002, ApJ, 575, 127
 Ishida M., Suzuki K., Someya K., 2007, JX-ISAS-SUZAKU-MEMO-2007-11, "Relative normalizations of XIS0-3 and PIN in revision 2 data"
 Ishisaki Y., et al., 2007, PASJ, 59, 113
 Kataoka J., et al., 2007, PASJ, 59, 279
 Laor A., 1991, ApJ, 376, 90
 Markowitz A., Edelson R., 2004, ApJ, 617, 939
 Miller J. M., Homan J., Steeghs D., Rupen M., Hunstead R. W., Wijnands R., Charles P. A., Fabian A. C., 2006, ApJ, 653, 525
 Miniutti G., Fabian A. C., 2006, MNRAS, 366, 115
 Miniutti G., Ballantyne D. R., Allen S. W., Fabian A. C., Ross R. R., 2006, MNRAS, 371, 283
 Mizuno T., 2007, JX-ISAS-SUZAKU-MEMO-2007-09, "HXD-PIN Background Model Reproducibility of v2 Products"

- Narayan R., Yi I., 1994, ApJ, 428, L13
Narayan R., Yi I., 1995, ApJ, 444, 231
Page K. L., Reeves J. N., O'Brien P. T., Turner M. J. L., 2005, MNRAS, 364, 195
Papadakis I. E., Petrucci P. O., Maraschi L., McHardy I. M., Uttley P., Haardt, F., 2002, ApJ, 573, 92
Pearson T. J., Blundell K. M., Riley J. M., Warner P. J., 1992, MNRAS, 259, 13
Rees M. J., Begelman M. C., Blandford R. D., Phinney E. S., 1982, Nature, 295, 17
Riley J. M., Warner P. J., Rawlings S., Saunders R., Pooley G. G., Eales S. A., 1989, MNRAS, 236, 13
Riley J. M., Warner P. J., 1990, MNRAS, 246, 1
Robinson A., Corbett E. A., Axon D. J., Young S., 1999, MNRAS, 305, 97
Ross R. R., Fabian A. C., 2005, MNRAS, 358, 211
Sambruna R. M., Eracleous M., Mushotzky R. F., 1999, ApJ, 526, 60
Saripalli L., Mack K.-H., 2007, MNRAS, 376, 1385
Türler M., et al., 2006, A&A, 451, L1
Tueller J., Mushotzky R. F., Barthelmy S., Cannizzo J. K., Gehrels N., Markwardt C. B., Skinner G. K., Winter L. M., 2008, ApJ, in press (astro-ph/0711.4130)
Vaughan S., Edelson R., Warwick R. S., Uttley P., 2003, MNRAS, 345, 1271
Vaughan S., Fabian A. C., Ballantyne D. R., De Rosa A., Piro L., Matt G., 2004, MNRAS, 351, 193
Woo J.-H., Urry C. M., 2002, ApJ, 579, 530
Wozniak P. R., Zdziarski A. A., Smith D., Madejski G. M., Johnson W. N., 1998, MNRAS, 299, 449